



Control of As and Ni releases from a uranium mill tailings neutralization circuit: Solution chemistry, mineralogy and geochemical modeling of laboratory study results

John Mahoney ^{a,*}, Maynard Slaughter ^b, Donald Langmuir ^c, John Rowson ^d

^a *MWH Americas, Inc., 1801 California Street, Denver, CO 80202, USA*

^b *Earth Science, University of Northern Colorado, Greeley, CO 80639, USA*

^c *Hydrochem Systems Corp., P.O. Box 23257, Silverthorne, CO 80498, USA*

^d *AREVA Resources Canada Inc., P.O. Box 9204, Saskatoon, SK, Canada S7K 3X5*

Received 17 October 2006; accepted 17 June 2007

Editorial handling by R. Fuge.
Available online 15 September 2007

Abstract

Processing U ores in the JEB Mill of the McClean Lake Operation in northern Saskatchewan produces spent leaching solutions (raffinates) with $\text{pH} \leq 1.5$, and As and Ni concentrations up to 6800 and 5200 mg L^{-1} , respectively. Bench-scale neutralization experiments ($\text{pH} 2\text{--}8$) were performed to help optimize the design of mill processes for reducing As and Ni concentrations in tailings and raffinates to $\leq 1 \text{ mg L}^{-1}$ prior to their disposal. Precipitate mineralogy determined by chemical analysis, XRD, SEM, EM, XM and EXAFS methods, included gypsum (the dominant precipitate), poorly crystalline scorodite (precipitated esp. from $\text{pH} 2\text{--}4$), annabergite, hydrobasaluminite, ferrihydrite, green rust II and theophrastite. The As was mostly in scorodite with smaller amounts in annabergite and trace As adsorbed and/or co-precipitated, probably by ferrihydrite. Geochemical modeling indicated that above $\text{pH} 2$, the ion activity product (IAP) of scorodite lies between the solubility products of amorphous and crystalline phases ($\log K_{\text{sp}} = -23.0$ and -25.83 , respectively). The IAP decreases with increasing pH , suggesting that the crystallinity of the scorodite increases with pH . Forward geochemical models support the assumption that during neutralization, particles of added base produce sharp local pH gradients and disequilibrium with bulk solutions, facilitating annabergite and theophrastite precipitation.

© 2007 Elsevier Ltd. All rights reserved.

1. Introduction

Predicting and controlling the mobility of contaminants such as As in groundwater becomes

increasingly important as risk assessment plays a greater role in the licensing and permitting of waste disposal facilities. Uranium ore from the Athabasca Basin of Northern Saskatchewan contains up to 10% As and 5% Ni by weight (Bourayne et al., 1999), and as a result of the extraction processes used to recover U, significant concentrations of As and Ni dissolve in the raffinate. In the JEB

* Corresponding author. Fax: +1 303 291 2221.
E-mail address: john.j.mahoney@mwhglobal.com (J. Mahoney).

Mill, U is extracted from the ore using H_2SO_4 . After U extraction, the leach residue solids are mixed with raffinate, commonly having $\text{pH} < 1.5$. Arsenic and Ni concentrations up to 6800 mg L^{-1} and 5200 mg L^{-1} have been quantified in some raffinates. Following neutralization, solids in the tailings slurry typically consist of 50–70% leach residue minerals with the remainder as precipitated phases. The leach residue contains unreacted quartz and illite, with lesser kaolinite and chlorite. Minor As and Ni also are present in residual niccolite (NiAs) and gersdorffite (NiAsS). The tailings slurry is pumped into the JEB Tailings Management Facility (TMF) for permanent disposal below the water table, using subaqueous emplacement (Bourayne et al., 1999). For facilities licensed by the Canadian Nuclear Safety Commission, federal and provincial Canadian regulators require that environmental effects of U mill tailings disposal on receiving waters remain acceptable over the very long term (greater than 10 ka). Based upon site-specific conditions, As concentrations of less than 5 mg/L for placed tailings pore waters were determined to be acceptable.

A goal of this study was to guide the design and operation of the tailings/raffinate neutralization circuit at the JEB Mill so as to minimize dissolved As and Ni concentrations in treated tailings before their disposal in the TMF. Laboratory studies conducted since 1997 (Langmuir et al., 1999a,b, 2006; Mahoney et al., 2005) show that As and Ni concentrations in neutralized raffinate can be minimized by implementing the following procedures. Prior to neutralization, the molar Fe/As ratio of the raffinate

is increased to ≥ 3 , (if necessary) by the addition of ferric sulfate in a flash mixing tank (Fig. 1). Previous studies have shown that As in neutralized solutions can be reduced to $1\text{--}2 \text{ mg L}^{-1}$ or less if, prior to neutralization, the molar Fe/As ratio is adjusted to ≥ 3 (Krause and Ettl, 1985; Harris and Monette, 1988; Harris and Krause, 1993; Langmuir et al., 1999a,b; Riveros et al., 2001). In the JEB Mill, after adjusting the Fe/As ratio, the combined raffinate and leach residue slurry is neutralized with lime to $\text{pH} 4$ in the first neutralization tank, and to $\text{pH} 7.0\text{--}7.5$, in the second neutralization tank (Fig. 1). Residence times in each tank are approximately 90 min. Laboratory work conducted prior to startup demonstrated that; (1) neutralization to $\text{pH} 4$ and a 90 min holding time in the first tank optimized the precipitation of As(V) in scorodite, and (2) a final $\text{pH} 7\text{--}8$ in the second tank reduced both Ni and As concentrations to 1 mg L^{-1} or less (Langmuir et al., 1999a,b).

A number of researchers have studied the mineralogy of arsenical mine tailings (cf. Foster et al., 1998; Roussel et al., 2000; Pichler et al., 2001; Paktunc et al., 1998, 2003, 2004; Moldovan et al., 2003; Moldovan and Hendry, 2005). Only Moldovan and Hendry (2005) considered the mineralogy of As in tailings during raffinate neutralization. However, in their mill-scale study of Rabbit Lake U mill tailings, their identification of scorodite and ferrihydrite was inferred from geochemical modeling calculations, not proven by mineralogical analysis. Based on modeling calculations they concluded that scorodite was precipitated between $\text{pH} 2.4$ and 3.1 , while from $\text{pH} 3.2$ to 11 , the scorodite presumably

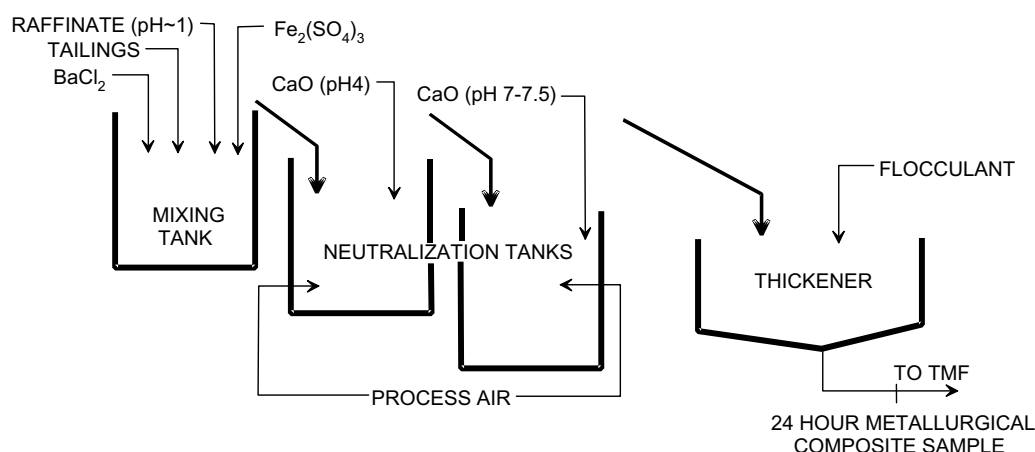


Fig. 1. Schematic diagram of the tailings neutralization circuit at the JEB Mill. The redox potential (Eh) in the mixing tank is approximately 660 mV.

dissolved and arsenate concentrations were controlled by its adsorption onto ferrihydrite. In the Rabbit Lake mill and in the tailings neutralization study of Moldovan and Hendry (2005), the pH is raised rapidly and continuously from pH 1–11 by the addition of lime ($\text{Ca}(\text{OH})_2$). As discussed below, this procedure does not favor the precipitation and crystallization or persistence of scorodite.

In this study, batch neutralization tests were performed from pH 2–8 using raffinate produced by the JEB U mill. The goals, most of which were original to this study, included to

- (1) evaluate the consequences of neutralizing the acid raffinates with NaOH versus with $\text{Ca}(\text{OH})_2$;
- (2) determine detailed changes in solution composition and mineralogy of precipitated solids as a function of increasing pH;
- (3) precipitate As and Ni-rich phases for quantitative mineralogical identification and characterization, using total chemical analysis, x-ray diffraction (XRD), scanning electron microscopy (SEM), electron microprobe (EM), x-ray microprobe (XM) and extended x-ray absorption fine structure (EXAFS) techniques;
- (4) determine the importance of As(III) and As(V) species in the neutralization process;
- (5) establish if the presence or absence of primary tailings solids (leach residue) from the leach circuit affects concentrations of As and Ni and the composition of solutions and secondary solids precipitated during neutralization and
- (6) develop a geochemical model that explains the changes in solution chemistry and secondary mineralogy as neutralization of the raffinate proceeds, including the precipitation and persistence of metastable phases, such as annabergite.

2. Experimental methods

2.1. Batch tests

In the first set of batch tests, approximately 60 L of Raffinate 1 (Table 1) was collected and spiked with As, Ni and Fe(III). A second set of tests utilized ~20 L of Raffinate 2, primarily to assess redox reactions. In both sets, the raffinate was spiked with

additional As as As_2O_5 (anhydrous), and Ni as $\text{NiSO}_4 \cdot 5\text{H}_2\text{O}$. Increasing the amounts of As- and Ni-bearing phases in the precipitated solids improved the reliability of their identification and characterization. Ferric sulfate (Triron[®] solution) was added to the raffinates to increase the Fe/As ratio.

Batch test experiments evaluated As and Ni behavior from pH 2 to ~8. Neutralizing agents included NaOH pellets, dry $\text{Ca}(\text{OH})_2$, and slaked lime ($\text{Ca}(\text{OH})_2 \cdot n\text{H}_2\text{O}$) slurry. Most tests used 2-L beakers as reaction vessels. Up to six 2-L beakers occupied a multi-jar tester (Fig. 2), with a 7th beaker, if needed, stirred separately. In the procedure, a neutralizing agent was added to all the beakers, while continuously stirring and monitoring pH. Larger amounts of base were added to successive beakers, so that each beaker attained its predetermined terminal pH, ranging from 2 to 8. After target pH values were reached, the slurries were filtered and the supernatant solutions analyzed.

2.2. Single-beaker test

To further concentrate As-bearing phases for mineralogical analysis, one experiment was performed in a container with ~5 L of spiked Raffinate 2. The neutralization procedure was similar to that used in the batch experiments, except that when the neutralized raffinate was filtered, the solution was returned to the beaker for additional neutralization and subsequent filtration. This procedure separated different solids as the pH increased by removing previously precipitated solids. Most significant was the removal of gypsum ($\text{CaSO}_4 \cdot 2\text{H}_2\text{O}$) accompanied by lesser amounts of scorodite ($\text{FeAsO}_4 \cdot 2\text{H}_2\text{O}$), precipitated at about pH 2. For the samples collected at pH > 2.2, aliquots of the raffinate were collected for laboratory analysis. Removal of solution for analysis reduced the total amount of raffinate available for subsequent neutralization. Samples of solids were collected at pH values of 2.17, 3.92, 5.66 and 7.34. Filtered samples of solution were taken at pH values of 3.92, 5.66 and 7.34. To increase the amount of solution and solids available during neutralization, a sample was not collected at pH 2.17, because an aliquot from the batch experiments taken at this pH (Sample 9-27-1, pH 2.18) was previously analyzed.

Table 1
Raffinate compositions and summary of Raffinate 2 slaked lime neutralization experimental results (concentrations in mg L⁻¹)

Parameter	Raffinates		Batch tests						Duplicates		Single beaker tests		
	Raffinate 1 Spiked	Raffinate 2 Spiked	9-27-1	9-27-2	9-27-3	9-27-4	9-27-5	9-27-6	9-28-A (duplicate of 9-27-5)	9-28-B (duplicate of 9-27-6)	SB-2	SB-3	SB-4
pH	1.5	0.97	2.18	3.23	4.09	5.29	6.24	7.32	6.08	7.37	3.92	5.66	7.34
Eh (mv)		670	640	590	460	280	140	-190	170	1.0	480	250	-200
Total As	732	690	150	14	3.6	1.15	0.56	0.39	0.76	0.45	6.04	2.1	0.34
As(III)		450	100	7	1.4	0.65	0.40	0.20	0.47	0.20	3.0	1.2	0.25
As(V)		220	48	7	2.0	0.46	0.16	0.17	0.29	0.24	2.9	0.92	0.10
Total Fe	2400	1850	1400	810	695	600	417	33	406	24	705	560	320
Fe(II)		685	540	460	460	390	330	26	320	20	450	440	280
Al	420	200	800	435	440	0.7	0.03	0.01	0.06	0.01	448	1.0	0.06
Ca	760	590	510	520	500	510	530	612	500	540	660	900	1000
Cl	14	13	16	18	19	20	17	18	19	22	16	19	19
Cu		19	16	15	15	1.2	0.03	0.01	0.01	0.11	15	1.3	0.07
K	210	360	390	640	745	570	403	477	160	210	200	260	240
Mg	260	230	1100	490	1010	50	380	750	340	310	340	440	640
Na	48	23	80	43	90	38	24	59	30	32	52	47	45
Si	260	190	580	330	240	62	20	8	19	4	180	58	26
Sulfate	14,100	21,400	10,200	7800	6500	4750	4400	3000	4000	3100	6900	5700	4900
Ni	560	515	500	480	460	370	240	13	230	13	470	380	230
Initial Fe/As	4.4	3.6											
Initial Fe/Ni	4.5	3.8											



Fig. 2. Experimental setup in the batch tests at near final pH values for Raffinate 1 neutralized with slaked lime. The pH values in beakers 1–5 from right to left were 2.18, 3.15, 4.04, 6.09 and 7.38.

3. Methods of chemical and mineralogical analysis

3.1. Solution analyses

Total concentrations of As, Fe and Ni were analyzed using a Perkin Elmer Optima Inductively Coupled Plasma (ICP) Optical Emission Spectrometer (OES). Spectral interference and background correction was accomplished by constructing a multicomponent spectral fitting model using Perkin Elmer software. For Al, Ca, K, Mg, Na and Si the samples were treated with 5% HNO₃ and analyzed directly using a sample injection system consisting of a Gem Cone Nebulizer, a Cyclonic Spray Chamber and a Lumina Injector. Ferrous iron was determined using a HACH Colorimetric Spectrophotometer with 1,10-phenanthroline as the colorimetric reagent. For the measurements involving Raffinate 2, an Amberlite IRA-900 anion exchange resin separated As(III) from As(V). Arsenic(III) and As(V) were individually analyzed by an ion chromatographic method (Tan and Dutrizac, 1985). Sulfate was measured gravimetrically using BaCl₂.

All pH readings were obtained with a Fisher Accumet Model 15 meter with an Accumet glass body single-junction Ag/AgCl combination electrode (4 m KCl). Redox potential (Eh) was measured during the Raffinate 2 batch tests using a Fisher Accumet Model 10 meter with a combination platinum Ag/AgCl reference electrode (4 m KCl). Calibration of pH was performed daily using pH 4.01 and 7.00 buffers. Redox electrodes were checked daily using quinhydrone in buffered solutions at pH values of 4.01 and 7.00. Eh values were corrected for reference electrode potentials. Chemical analyses of the raffinate solutions used in the batch and single bea-

ker tests, and the experimental results of the tests are given in Table 1.

3.2. Mineralogical analyses

Chemical analyses of solids, except for S, organic C and water, were done by the University of Colorado Mineral Analysis Laboratory using ICP emission spectrometry following HCl and HNO₃ digestion. Sulfur was analyzed using a Leco Sulfur Analyzer (model S144DR) by ASTM method D4239. Organic C was analyzed using a Leco Carbon Analyzer (model CR12) by ASTM method D5373 (American Society for Testing and Materials, 2005), concentrations were commonly on the order of 0.01% or less for organic C. Water was determined by weight loss on heating. H₂O⁻ was measured as water loss at 70 °C. H₂O⁺ was determined as water loss above 70 °C at 100 °C intervals to 900 °C to insure that there was no weight gain due to oxidation of iron. Iron(II) analyses were conducted using a hot digestion in HF and H₂SO₄, followed by a dissolving solution of boric and phosphoric acids, and a potassium dichromate titration using Na diphenylamine sulfonate as an indicator. Analyses were done in triplicate and averaged. For the Raffinate 2 solids, Fe(II) analyses were performed on the damp samples immediately after filtration to avoid Fe oxidation.

Mineralogical testing included X-ray diffraction (XRD) of powdered samples using a Scintag diffractometer employing Cu K α radiation. Each sample was scanned at 2°/min from 2° 2 θ to 70° 2 θ . In the analysis of diffraction patterns, scans were presented with a maximum intensity of 200 counts s⁻¹, to eliminate the upper portions of gypsum diffractions and to emphasize weak diffractions of the

always minor amounts of poorly crystalline phases precipitated from the raffinate. Scanning electron microscopy (SEM) with energy dispersive analysis was performed on select samples using a JEOL Electron Microscope, and analyzed for As, Ni, Fe, S, Al, Si, Mg and Ca. Sample powders were mounted on standard (Au-coated) EM cylinders. Qualitative EM and XM scans at Argonne National Laboratory's Advanced Photon Source supplemented the SEM analyses. The XM slides were mounted dry on glass slides.

Quantitative mineralogical analyses of all samples were performed using the computer model QMAS (Slaughter, 1985, 1990), which combines the XRD, EM and XM results and sample chemistry using linear programming. In the QMAS model, sets of linear inequalities optimize linear “objective functions” to determine approximate mineral compositions and mineral amounts. The inequalities are of either \geq or \leq kinds. One may specify an objective function and inequalities for each type of analysis, whether by x-ray diffraction, optical, infrared, chemical and/or other method. Mineral Gibbs free energies of formation may also be used in the

inequalities, with specified ranges of mineral compositions. The objective functions and sets of inequalities may be combined. The QMAS method determines approximate chemical compositions of selected minerals including scorodite, annabergite ($\text{Ni}_3(\text{AsO}_4)_2 \cdot 8\text{H}_2\text{O}$), ferrihydrite ($\text{Fe}_2\text{O}_3 \cdot 0.5\text{H}_2\text{O}$), theophrastite ($\gamma\text{-Ni}(\text{OH})_2$) and basaluminite ($\text{Al}_4\text{SO}_4(\text{OH})_{10} \cdot n\text{H}_2\text{O}$; $n = 2$ to 13).

4. Results and discussion

4.1. Mineralogical results

Mineralogical analyses of Raffinate 2 batch and single beaker test precipitates are summarized in Tables 2 and 3 as quantified by the QMAS program. Table 2 shows the dominance of gypsum and the later “dilution” of phases such as early forming scorodite, as other phases (mainly ferrihydrite and basaluminite) precipitate with increasing pH. The basaluminite has a composition between hydrobasaluminite (36 H_2O) and basaluminite (10 H_2O). The mineralogical analyses provided both qualitative and quantitative evidence of changes in the

Table 2
Mineral composition (wt%) of solids from slaked lime neutralization of Raffinate 2 in batch tests

Sample no.	9-27-1	9-27-2	9-27-2 (duplicate)	9-27-3	9-27-4	9-27-5	9-27-6	9-28-A	9-28-B
pH	2.18	3.23	3.23	4.09	5.29	6.24	7.32	6.08	7.34
Amorphous Silica	0.06	0.2	0.2	0.81	1.3	1.52	1.53	1.51	1.46
Rutile	0.09	0.08	0.08	0.07	0.06	0.06	0.05	0.07	0.05
Basaluminite	0.03	0.07	0.06	1.6	5.3	4.7	4.4	5.8	4.4
Ferrihydrite	0	0	0	0	2.4	2.6	3.7	3.9	2.9
Goethite	0	2.8	2.6	2	0.34	0	0	0	0
Gypsum	83	80	77	77	76	75	74	68	71
Ca(OH) ₂	2.2	1.7	3.0	1.6	0.07	0.23	0.34	1.8	1.9
Theophrastite	0	0	0	0	0.3	1.2	2.3	1.2	2.4
Jarosite	0.04	1.1	1.1	2.2	1	0.9	0.85	1.1	0.9
Annabergite	0	0	0.04	0.17	0.58	0.47	0.29	0.63	0.31
Scorodite	6.5	6.8	7.2	5.7	5.0	4.6	4.4	7.9	6.2
Strengite	1.9	2.0	2.3	1.8	1.6	1.6	1.4	1.8	1.5
Quenstedtite	6.1	5.5	5.9	6.8	6.3	6.8	7.0	7.1	7.2
Total (wt%)	99.98	99.98	99.96	99.95	99.98	99.97	99.95	99.97	99.99
Normalized concentrations (wt%) without gypsum, Ca(OH) ₂ or quenstedtite									
Amorphous Silica	0.7	1.8	1.4	5.6	7.3	8.6	8.0	6.5	7.3
Rutile	1.04	0.61	0.59	0.48	0.34	0.34	0.26	0.30	0.25
Basaluminite	0.4	0.5	0.4	11	29	26	23	25	22
Ferrihydrite	0	0	0	0	13.	15	20	12.9	15
Goethite	0.00	21	19	14	1.9	0	0	0	0
Theophrastite	0.00	0.00	0.00	0.00	1.9	6.7	12.	5.5	12
Jarosite	0.46	8.4	8.2	15	5.6	5.2	4.5	4.9	4.3
Annabergite	0.00	0.00	0.29	1.2	3.2	2.7	1.5	2.7	1.6
Scorodite	76	52	53	40	28	26	23	34	31
Strengite	22	16	17	13	9.1	8.9	7.5	8.0	7.3

composition and mineralogy of the solids formed during neutralization. These changes are visually apparent in Fig. 2, which shows slaked lime neutralized Raffinate 1 suspensions near their final pH values.

In the neutralization of Raffinate 2, an olive green color was present in the higher pH samples (Fig. 2). High Fe(II) concentrations were found in the samples collected at pH > 7. X-ray diffraction of precipitates from Raffinate 2 batch test samples 9-27-6 and 9-28-B (Table 2) gave a diffraction peak at 8.7° 2θ, suggesting a phase intermediate between green rust II and ferrihydrite. This peak is a shift from the 8.1° 2θ (001) diffraction of green rust II. Single beaker sample SB#4 collected at pH 7.34 (Table 3) shows diffractions of green rust II shifting to an intermediate phase, then becoming true ferrihydrite. Upon drying, the intermediate phase has an orange brown color, although not all the Fe(II) has oxidized. The mineral fougérite [(Fe²⁺, Mg)₆Fe₂³⁺(OH)₁₈ · 4H₂O] is noted in one single beaker sample. Its presence is due in part to

the availability of substituent Fe(II). Fougérite occurs in the same pH range as goethite and “iron oxide hydrate” (JCPDS #13-92 (JCPDS, 2005)). Fougérite is an oxyhydroxide with a hydration state slightly greater than one, with diffractions near those of ferrihydrite, but suggestive of incipient “green rust II”.

Goethite (α-FeOOH), also precipitates beginning at pH ~ 2.5 to 3, where it is identified by X-ray diffraction. The goethite forms coatings on lime particles that are most obvious when dry Ca(OH)₂ is used as the base, but they are also noted when slaked lime slurry is used. As the pH increases, the goethite visibly dissolves from the beakers and is replaced by ferrihydrite and “green rust II” as indicated by the diffraction data. The raffinate solids suspended in solution at pH 7.4 (Fig. 2) have a deep olive green color, and a lighter olive green color at pH 6.09 consistent with the presence of “green rust II”. The deep olive green color suggests that Fe(II) partially substitutes for Fe(III). In the experiments with Raffinate 1, the solids were allowed to air dry before analysis. This resulted in additional Fe(II) oxidation. Ferrihydrite was the dominant solid in all samples formed at pH > 6, in which FeO was still present in the ferrihydrite, as evidenced by chemical analysis, the green color, and shifted high angle diffractions. Jarosite (KFe₃³⁺(SO₄)₂(OH)₆) occurs in most samples with Na partially substituting for K. The jarosite usually precipitates with goethite at low pH, with maximum precipitation around pH 4 to 4.5. Some phases, most notably quenstedtite (Fe₂(SO₄)₃·11H₂O), were found in the experiments, but are not present in the tailings at the JEB TMF. Quenstedtite is an evaporation product that formed because the filter cakes could not be thoroughly washed after filtration.

Fig. 3 shows the mineralogical composition of the As, Ni and Fe bearing phases in the single beaker tests, normalized after removal of gypsum, quenstedtite and unreacted Ca(OH)₂. The figure shows that scorodite is the dominant As-bearing precipitate at pH 2.17. At pH 3.9, scorodite precipitation is completed and Fe-bearing phases (dominantly fougérite but probably including ferrihydrite) start to form. Sample SB-3 (pH 5.66) shows increasingly smaller proportions of the Fe-bearing minerals because of their dilution by precipitating basaluminite (Table 3; not shown on the figure) and initial formation of theophrastrate. Ferrihydrite and theophrastrate dominate the composition of the final sample (SB-4) at pH = 7.34.

Table 3
Mineral composition (wt%) of solids from slaked lime neutralization of Raffinate 2 in Single beaker tests

Sample no.	SB#1	SB#2	SB#3	SB#4
pH	2.17	3.92	5.66	7.34
Amorphous Silica	0.14	1.3	3.10	3.10
Rutile	0.08	0.05	0	0.01
Basaluminite	0.05	8.3	29.	0.91
Ferrihydrite	0	0	0.16	47
Fougérite	0	18.1	0	0
Gypsum	77	25	478	11.
Ca(OH) ₂	0.66	3.8	3.0	1.61
Theophrastrate	0	0	3.4	35
Jarosite	0.19	13	0.09	0.02
Annabergite	0.13	3.3	0.18	0.64
Scorodite	10	7.6	0.07	0.14
Strengite	2.1	3.2	0.07	0.06
Quenstedtite	9.3	16	13	0.76
Total (wt. %)	100	99.79	99.95	99.98

Normalized concentrations (wt%) without gypsum, Ca(OH)₂ or quenstedtite

Amorphous Silica	1.1	2.3	8.6	3.6
Rutile	0.63	0.09	0	0.01
Basaluminite	0.39	15	80	1.0
Ferrihydrite	0	0	0.44	54
Fougérite	0	33	0	0
Theophrastrate	0	0	9.3	40.3
Jarosite	1.5	24	0.25	0.02
Annabergite	1.0	6.0	0.49	0.74
Scorodite	79	14	0.19	0.16
Strengite	16	5.9	0.19	0.07

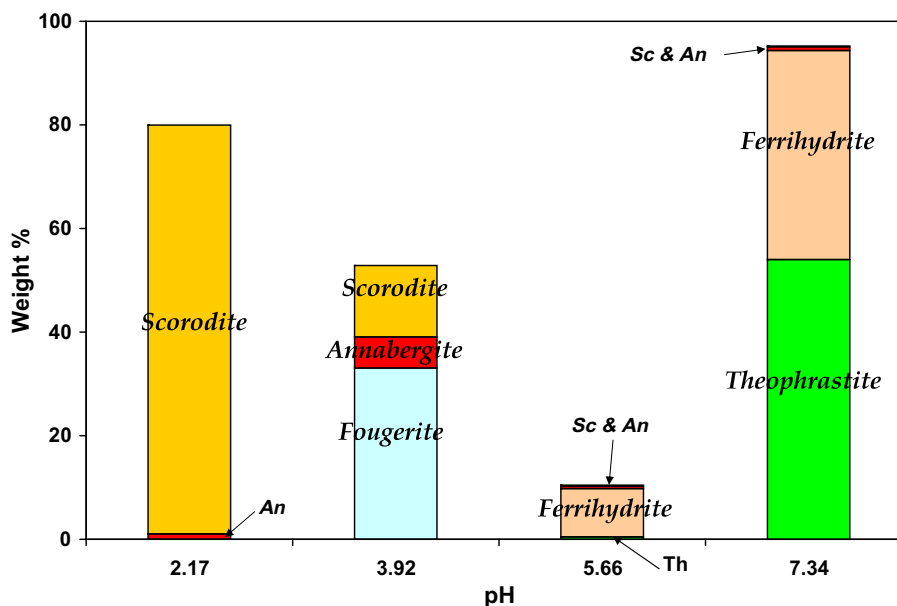


Fig. 3. Relative weight percent values of minerals precipitated in the single beaker tests using lime and Raffinate 2 with final pH values of 2.17, 3.92, 5.66 and 7.34. Weight percent values have been normalized by subtracting the amounts of gypsum, quenstedtite and unreacted $\text{Ca}(\text{OH})_2$. Abbreviations are annabergite, An; scorodite, Sc; and theophrastite, Th. See Table 3.

No significant increase in As concentrations is observed with increasing pH, suggesting that precipitated scorodite remains insoluble as the pH increases to at least 7.4. The scorodite contains Ni^{2+} and Fe(II) substituting for Fe(III). With increasing pH, Ni(II) substitution for Fe(III) increases, while Fe(II) substitution decreases. SEM, EM and XM elemental scans show Ni intimately integrated in the scorodite phases from samples collected at $\text{pH} < 4$, but especially in the pH 2.17 sample. An exhaustive EXAFS study (Chen, 2006) concluded that the As in scorodite, which is normally 4-fold oxygen coordinated, has a coordination number slightly less than 4 in these samples. Substitution of Ni(II) and Fe(II) for Fe(III) most likely has reduced the domain size, effectively reducing the As coordination number. A broad scorodite diffraction peak at $28\text{--}29^\circ 2\theta$ and a second characteristic scorodite diffraction peak at $19.8^\circ\text{--}19.9^\circ 2\theta$ persisted and did not change with changing pH or with time. Analysis of aged samples from the mill that had undergone acid dissolution to selectively remove gypsum showed that the acid did not completely remove Ni, demonstrating that Ni is present in an acid insoluble phase (i.e. in scorodite). Aluminum, limited to 2 mole % of Fe(III) in the scorodite, occupies octahedral sites. A separate study of solids from the TMF, as well as solids stored as part of a series of laboratory aging tests (nominal pH of 7 to

7.5, room temperature) indicated that the scorodite persists and remains poorly crystalline for at least several years.

During the initial neutralization of the raffinate, Ni precipitates mainly as a substituent in scorodite or other Fe-bearing phases. Some annabergite also forms as a result of the pH gradients between the bulk raffinate solution and particles of added $\text{Ca}(\text{OH})_2$. With increasing pH, Ni precipitates as a highly disordered Ni–Mg hydroxide, resembling poorly crystalline theophrastite with substituent Mg.

4.2. Arsenic, nickel and iron concentrations

Concentrations of total As versus pH in all of the neutralization experiments are shown in Fig. 4. Results for the different experiments are generally similar. However, experiments that used Raffinate 2 show higher As concentrations in the higher pH ranges, probably resulting from the smaller Fe/As ratio in Raffinate 2 (Table 1). Fig. 4 includes data sets using slaked lime or NaOH as neutralizing agents. The presence of leach residue and the choice of neutralizing agent evidently have no effect on final As concentrations. The continuously decreasing As concentrations, and the similarity of the As concentrations between the Raffinate 2 batch

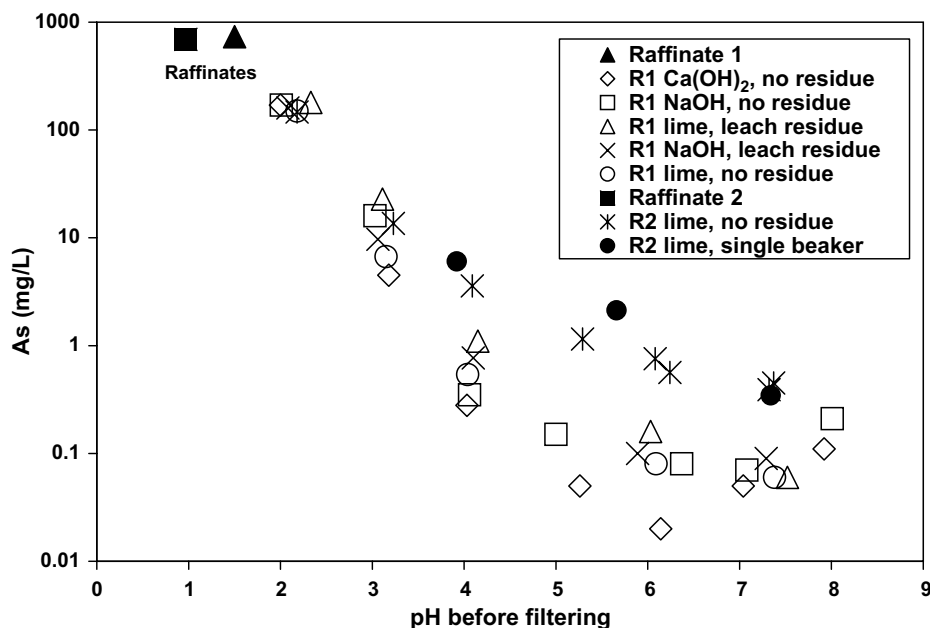


Fig. 4. Total As concentrations as a function of pH in all of the raffinate neutralization experiments. Raffinate 1 (R1) and Raffinate 2 (R2) are shown as a solid triangle and solid square, respectively. Experiments were performed with and without mineral leach residues, and used lime (CaO), slaked lime (Ca(OH)₂), or NaOH as added bases.

measurements, which contained accumulated secondary solids, and the single-beaker measurements, in which solids were removed as precipitation proceeded, indicates that once precipitated, the solids that contain As do not react (re-equilibrate) further with the solutions.

Fig. 5 shows Ni concentrations as a function of pH, and indicates that the choice of neutralizing agents does not influence Ni concentrations in the batch tests. Unlike the effect of the Fe/As ratio on As concentrations, differences in the Fe/Ni ratio do not significantly affect Ni concentrations at near

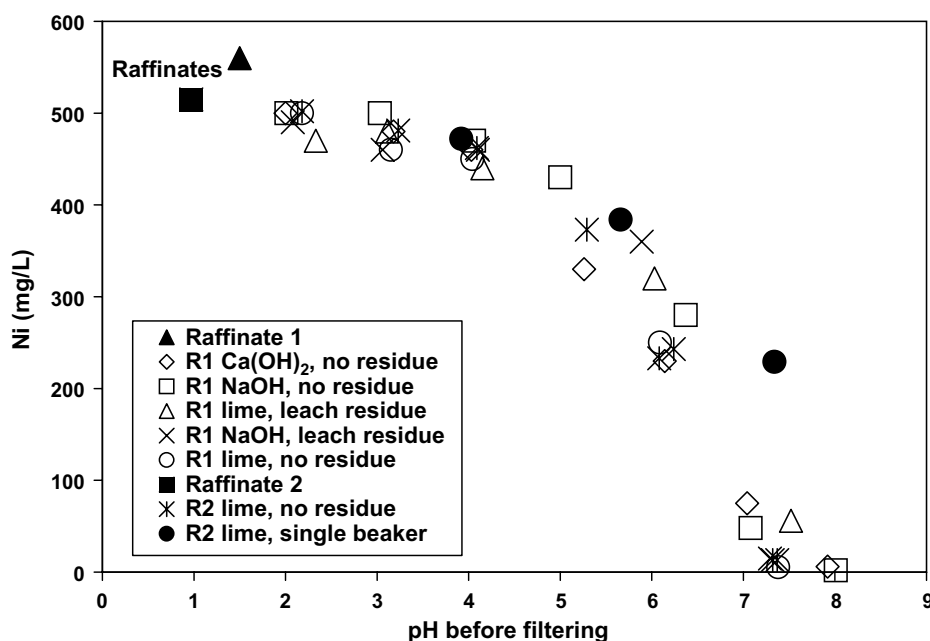


Fig. 5. Nickel concentrations as a function of pH in all of the raffinate neutralization experiments. Raffinate 1 (R1) and Raffinate 2 (R2) are shown as a solid triangle and solid square, respectively. Experiments were performed with and without mineral leach residues, and used lime (CaO), slaked lime (Ca(OH)₂), or NaOH as added bases.

terminal pH values. However, the 3 samples from the single-beaker experiment have greater Ni concentrations than were found in the batch tests, particularly at higher pH values. Fig. 6 shows total As, total Fe, Fe(II) and Ni concentrations during Raffinate 2 neutralization, and demonstrates a correlation between Ni and Fe(II). At comparable pH values, Ni and Fe(II) concentrations tend to be greater in the single-beaker tests than in the batch tests. Removal of previously precipitated solids capable of adsorbing Ni may explain the greater Ni concentrations in the single-beaker tests.

Fig. 7 shows moles of As, total Fe, Ni and Fe(II) removed from solution as neutralization proceeds in the Raffinate 2 batch tests. The molar amounts shown at pH of 2.18 represent the change in composition from the un-neutralized raffinate at pH 0.97. Precipitated amounts in Fig. 7 are cumulative changes. Thus, the data shown at pH 5.29, for example, represent changes from pH 0.97 to pH 5.29. At pH 7.32, essentially all of the Fe and As and most of the Ni have been removed. The amount

removed roughly equals the composition of the original raffinate. Iron and As are removed in a 1/1 ratio up to pH 2.18; strong evidence for scorodite precipitation under these conditions. Continued removal of As in scorodite beyond pH 2.18 is supported by mineralogical analyses of the single-beaker precipitates. As the pH increases to 3.23 most of the remaining As is removed, probably still as scorodite. Approximately 98% of the total As and a significant amount of the Fe is in the solids by pH 3.23.

At low pH, small amounts of Ni are precipitated in annabergite. This is because of strong pH gradients and local pH values that exceed 10 near added particles of slaked lime. Coupled with the abundance of As and Ni, this allows the formation of annabergite. Nevertheless, saturation index (SI) calculations indicate that annabergite is substantially undersaturated in the bulk solution. The SEM, EM and XM work described above, indicate that some Ni is incorporated in rapidly precipitating scorodite. With increasing pH (pH > 5) following complete removal of the As, the remaining Ni precipitates in theophorite.

The batch and single beaker tests show that a variety of secondary As, Fe and Ni phases precipitate during the neutralization of acid raffinate solutions. With increasing pH these include scorodite, ferrihydrite and theophorite. Among the metastable phases, goethite and fougurite disappear with increasing pH, whereas annabergite persists at pH values above 7. A raffinate Fe/As ratio of ≥ 3 reduces the As concentrations resulting from neutralization to less than 1 mg/L and apparently stabilizes scorodite up to pH values above 7 (cf. Mahoney et al., 2005).

4.3. Redox concepts

There are several ways to assess oxidation–reduction conditions during neutralization, although they generally give different answers. One of the simplest methods is to measure the Eh of the system with a Pt or other indicator electrode and a reference electrode (Macalady et al., 1990). However, in a system such as the raffinate, the measured Eh is a total voltage resulting from the combined effect of multiple electron transfer reactions, many of which are poorly reversible. These involve the redox pairs As(V)/As(III), Fe(III)/Fe(II), and the redox sensitive elements Mn, C, S and N, among others. Because the measured Eh is the sum of potentials generated by

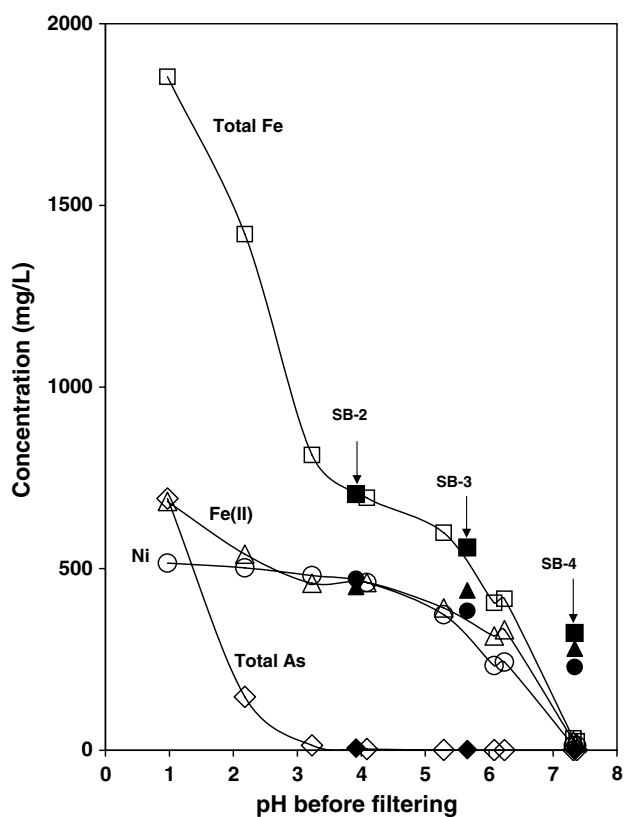


Fig. 6. Arsenic, Ni, total Fe and Fe(II) concentrations during slaked-lime neutralization of Raffinate 2. Squares denote total Fe, diamonds As, circles Ni, and triangles Fe(II) concentrations. Filled symbols are single beaker (SB) results. Solid curves connect results of the 9–27 batch experiments. See Table 1.

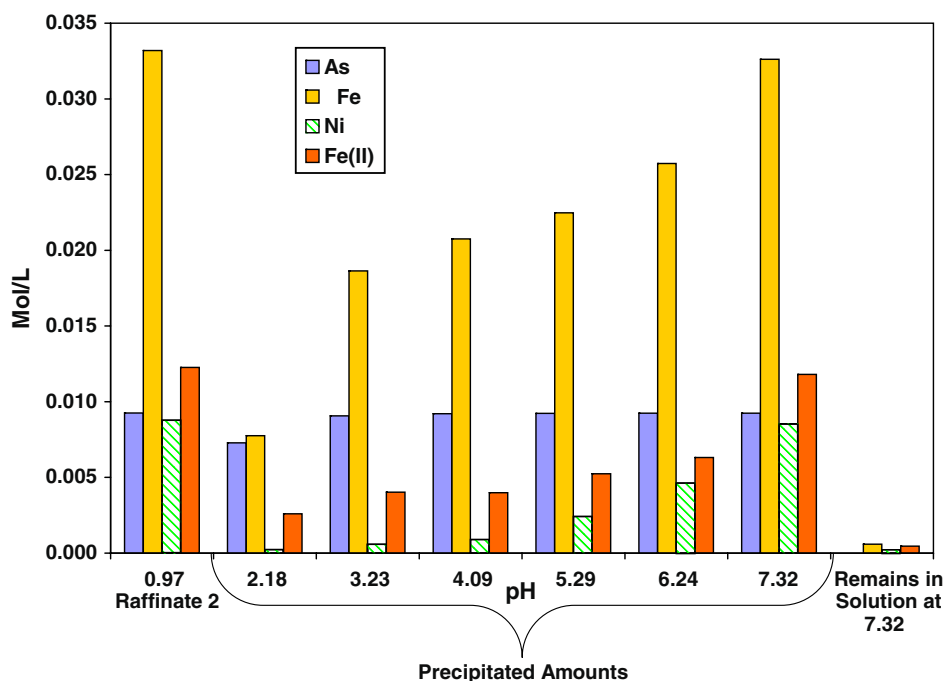


Fig. 7. Molar concentrations in the Raffinate 2 batch neutralization experiments involving added slaked lime. Shown are dissolved molar concentrations in the raffinate, molar amounts precipitated in experiments from pH 2.18 to 7.32, and molar amounts remaining in solution at pH 7.32. Precipitated amounts are based on differences in concentrations in the raffinate and in respective neutralized solutions.

more than one redox reaction, and these reactions are usually not in equilibrium with each other, it is termed a mixed potential (Stumm and Morgan, 1996). Given the probability that the measured Eh is a mixed potential, it is important also to compute apparent Eh values from the measured concentrations of the species in individual redox couples.

4.4. Redox conditions

In the experiments, three types of redox determinations were made. First, nearly continuous Eh measurements were obtained using a Pt indicator electrode and a reference electrode. Samples also were analyzed for total As, and separately for their As(III) and As(V) concentrations. Total Fe and Fe(II) concentrations also were measured, with Fe(III) calculated by difference. Fig. 8 is a plot of the measured Eh, as well as Eh values computed separately from the concentrations of Fe and As species using PHREEQC (Parkhurst and Appelo, 1999). Measured Eh values are generally less than the values computed from the Fe pair, and greater than the values computed from the As pair, possibly indicating that the measured Eh is a mixed potential. Given the general disagreement between Eh values computed from concentrations of Fe and As redox pairs

and the measured Eh, calculations of As(V) speciation and the saturation state of arsenate and Fe(III) minerals were performed using measured concentrations of total As(V) and Fe(III), and not the Eh. Table 1 shows that concentrations of the reduced As and Fe species are comparable to those of the oxidized species, regardless of pH. Although this is true in this study and in mill processing, evidence from laboratory aging tests and from the pore waters of buried tailings in the TMF after 5a of aging indicates that ultimately the system becomes fully oxidized with As(V) and Fe(III) species dominating in the pore water and in the solids.

4.5. Arsenate speciation

Arsenate speciation as a function of pH was computed with PHREEQC for the Raffinate 2 data (Table 1) using measured total Fe(III) and As(V) concentrations. Fig. 9 shows that with increasing pH the dominant arsenate species are H_3AsO_4 , FeHAsO_4^+ , and FeAsO_4 .

4.6. Eh–pH relations

Fig. 10 shows the theoretical stability fields of aqueous Fe species and $\text{Fe}(\text{OH})_3(\text{s})$ in the system

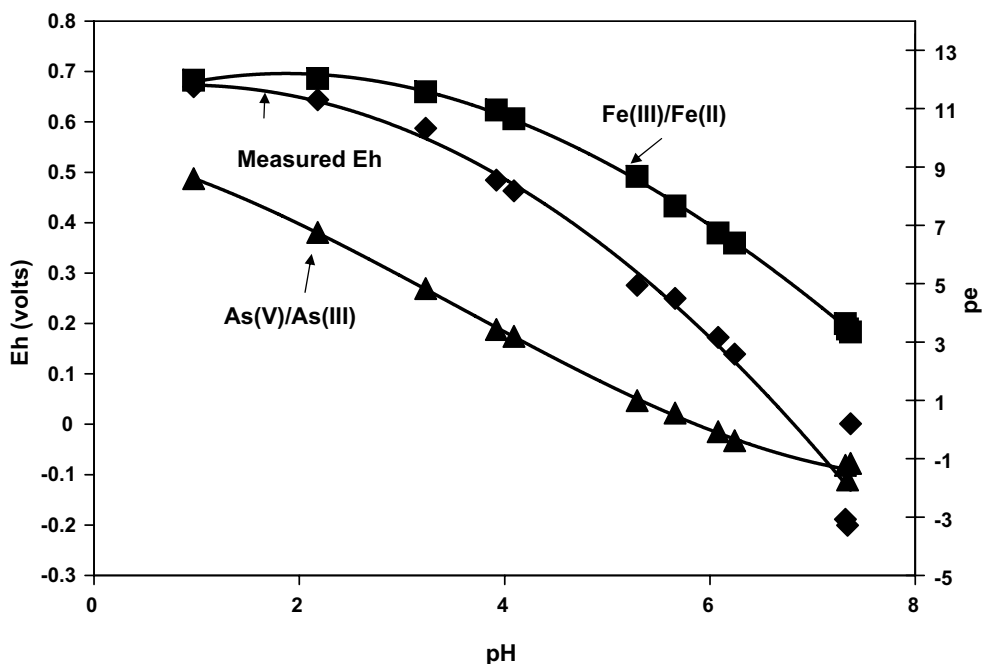


Fig. 8. Measured Eh values and Eh values computed from the concentrations of Fe and As redox species measured during neutralization of Raffinate 2 with slaked lime.

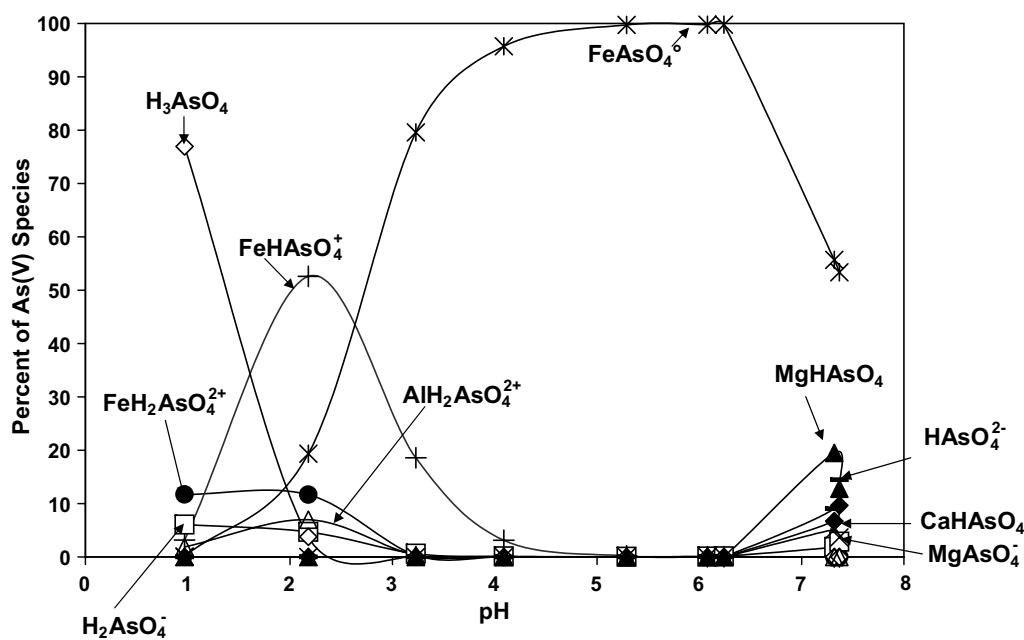


Fig. 9. Percent distribution of As(V) aqueous complexes in batch experiments during neutralization of Raffinate 2 with slaked lime. The figure is computed with PHREEQC, based on the chemical analytical data in Table 1. The Fe and As concentrations used in the calculations are the Fe(III) and As(V) chemical analyses from Table 1.

Fe–H–O–CO₂–S at concentrations typical of the raffinate neutralization experiments and the mill neutralization circuit. Also shown are Eh values computed from measured Fe concentrations, which decrease generally during neutralization particularly

above pH 4. The Eh values, which are based on the activities of free Fe²⁺ and Fe³⁺ ions, were calculated with PHREEQC from the Fe(II) and Fe(III) concentrations. The high SO₄²⁻ concentration (0.1 mol L⁻¹), which is a typical value for the

raffinates, lowers the activity of free Fe^{3+} ion to about 0.1% of the total Fe(III) concentration, and preferentially complexes Fe^{3+} over Fe^{2+} . This reduces the Eh boundary for the $\text{Fe}^{3+} + \text{e}^- = \text{Fe}^{2+}$ reaction from 0.77 V to 0.69 V, so that the first 5 data points plot on the boundary between the Fe(III) and Fe(II) species fields in Fig. 10.

5. Geochemical modeling

5.1. Overview

Geochemical modeling using PHREEQC (Parkhurst and Appelo, 1999) was used to confirm the reactions that control As and Ni behavior during slaked lime neutralization of Raffinate 2. Modeling calculations used an updated thermodynamic data base for metal arsenate complexes and amorphous and crystalline scorodite (Langmuir et al., 2006), the primary source of the database was the WATEQ4F.DAT file provided with the program.

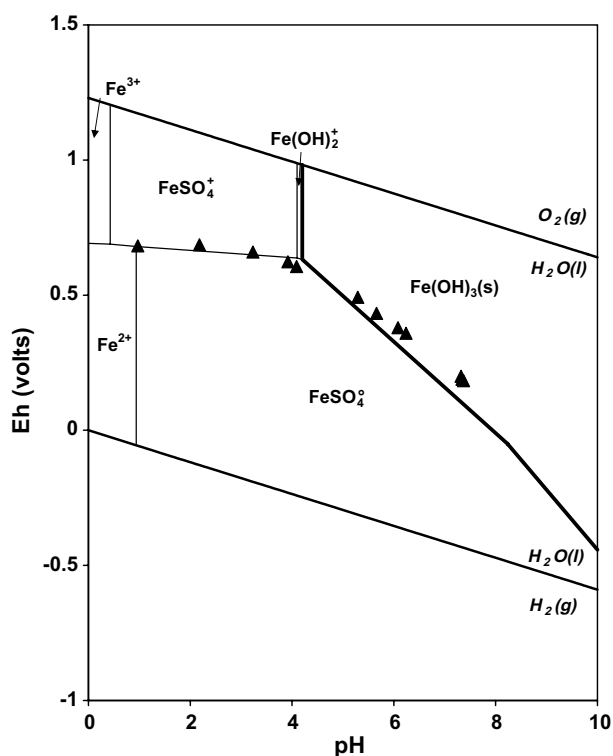


Fig. 10. Theoretical Eh–pH diagram for the system Fe–O–H–S–CO₂ neglecting sulfide aqueous species and solids. Triangles denote Eh values computed with PHREEQC from measured Fe(III) and Fe(II) concentrations. The Fe(OH)₃(s)/solution boundary is drawn (in bold) for a dissolved Fe concentration of $10^{-5} \text{ mol L}^{-1}$. The solution contains $\text{SO}_4^{2-} = 0.1 \text{ mol L}^{-1}$ and $\text{HCO}_3^- = 10^{-2.7} \text{ mol L}^{-1}$.

Pertinent reactions can be reviewed in the supplementary information available from the publisher's website. Redox conditions were defined by Eh measurements, and separately by the Eh values computed using PHREEQC from measured concentrations of Fe(III) and Fe(II), and As(V) and As(III) species. A forward geochemical model was also developed to explain the precipitation of metastable annabergite and theophrastite from low-pH solutions.

5.2. Saturation Index Calculations

PHREEQC (Parkhurst and Appelo, 1999) was used to calculate saturation indices (SI values), which are defined as

$$\text{SI} = \log \frac{(\text{IAP})}{(K_{\text{sp}})}$$

where IAP is the ion activity product of the mineral, and K_{sp} is the solubility product constant. At a saturation index of 0.0, the IAP equals the K_{sp} and the mineral is at equilibrium with the solution. Positive values mean that the solution is supersaturated with respect to the mineral. Barring kinetic constraints, the mineral should then precipitate and concentrations in solution should decrease. Negative SI values mean that the solution is undersaturated and the mineral, if present, should dissolve.

Saturation indices of minerals containing Fe(III) and As(V) were computed using the measured concentrations of these species (Table 1). Fig. 11 shows PHREEQC-computed SI values for amorphous ferric arsenate and crystalline scorodite, ferrihydrite, theophrastite and annabergite. Based on the SI calculations, gypsum (not shown) is at equilibrium with the solution at all pH values, with an average SI value of 0.05 ± 0.13 . Saturation with respect to gypsum has been a consistent condition in all solutions including in pore water samples collected from the TMF, and has thus been used as a confirmation that Ca and SO₄ chemical analyses and gypsum SI calculations are correct. As pH values increased, ionic strengths decreased from 0.3 to approximately 0.1 molal. PHREEQC uses the Davies Equation to calculate ion activity coefficients, which for this range of ionic strengths is an appropriate choice.

Fig. 11 shows that during neutralization the SI of scorodite(cr) decreases from highly supersaturated values (SI $\sim +2$ to $+3$) between pH 1.5 to 3, to SI $\sim +1$ at pH 7.4. Saturation indices for ferric

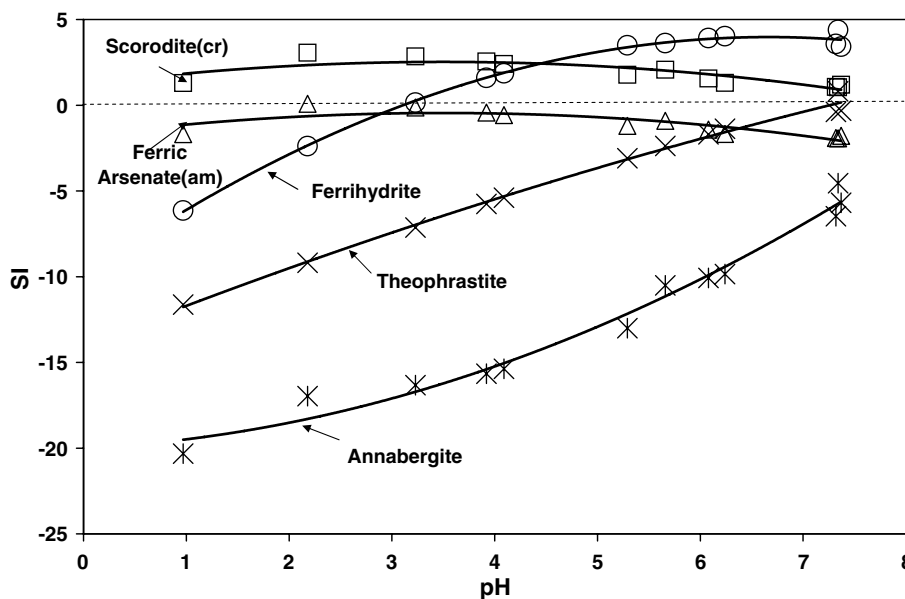


Fig. 11. Saturation indices of some important minerals as a function of pH during neutralization of acid raffinate with slaked lime in batch experiments. The Fe and As concentrations input into the PHREEQC model are the measured concentrations of Fe(III) and As(V) from Table 1.

arsenate(am) indicate that it is near equilibrium with the solution up to $\text{pH} \sim 3$, but becomes progressively undersaturated at higher pH values. Such behavior is consistent with an amorphous ferric arsenate (or poorly crystalline scorodite) being replaced by more crystalline scorodite (less soluble) material as the pH increases to 7.4. This trend suggests that the solubility product of precipitated scorodite decreases with increasing pH. There is a logical reason for such behavior (Langmuir, 1997). Because of decreasing concentrations of dissolved Fe(III) and As(V) with increasing pH, the rate of precipitation of scorodite must decrease. This should produce a more crystalline (ordered) phase. Also, with increasing pH, relatively amorphous scorodite becomes undersaturated and should preferentially dissolve, leaving the more crystalline fraction behind. Any released As is then reprecipitated in more crystalline scorodite. This may be a result of Ostwald ripening (Langmuir, 1997).

The SI of ferrihydrite (HFO) as $\text{Fe}(\text{OH})_3$ ($\text{p}K_{\text{sp}} = 37.1$) in Fig. 11 increases from undersaturated values below $\text{pH} 3\text{--}5$, to substantially supersaturated values above this pH. The supersaturated values for HFO probably reflect the slow kinetics of its precipitation and crystallization, because of the elevated sulfate and arsenate concentrations in these solutions (Langmuir et al., 2006). SI values for theophrastite show that it is generally undersaturated, but attains saturation at

$\text{pH} 7.4$. Annabergite is always undersaturated in the neutralization experiments.

5.3. Forward geochemical modeling

Forward geochemical models were developed to simulate the processes that take place during neutralization. It was found that different models can produce similar results. Most importantly the models help explain the precipitation of minerals that cannot be explained by equilibrium-based geochemical modeling. The models were designed primarily to explain changes in As, Ni and Fe concentrations, with an emphasis on As and Ni behavior. First, a geochemical model that assumed equilibrium with the bulk solution was developed to reproduce the precipitation of gypsum, scorodite and theophrastite. Calcium and SO_4 were assumed to be controlled by gypsum precipitation, consistent with its abundance and near-zero saturation indices. Aluminum was assigned to basaluminite. The decrease in Ni concentrations with increasing pH required inclusion of a modeling step to precipitate increasing amounts of annabergite, in spite of the fact that annabergite remains undersaturated in the bulk solutions. Accordingly, the modeling addressed localized precipitation of the Ni arsenates by assuming locally higher pH values out of equilibrium with the bulk solution, such that annabergite could precipitate. Model assumptions were tested by

matching computed and measured concentrations of As, Ni, SO_4 , Al and Fe to the experimental results.

5.4. Modeling Details

Initial modeling simulations assumed equilibrium conditions. In the initial models, $\text{Ca}(\text{OH})_2(\text{s})$ was added to the raffinate at pH 0.97 to raise its pH in single steps to 2.18, 3.23, 4.09 and 5.29, respectively. At each final pH, minerals that had become supersaturated were allowed to precipitate.

To improve the fit between measured and modeled As concentrations, increasingly negative $\log K_{\text{sp}}$ values for poorly crystalline scorodite were assumed with increasing pH, as suggested by the foregoing discussion (Fig. 11, Table 4). Redox conditions were based upon the Eh measurements. The Eh values were included because the model required a mechanism to oxidize the As(III) to As(V). PHREEQC cannot use separate redox conditions for Fe and As, so measured Eh values provided a reasonable compromise. With adjustments to the K_{sp} for scorodite, the simple equilibrium model did an excellent job of matching measured As and Fe concentrations. However, this model did not reproduce Ni concentrations, particularly at low pH.

To match observed Ni concentrations, a non-equilibrium step was added, in which a portion of the raffinate is neutralized to pH 7 without allowing scorodite to precipitate. This step reflects the disequilibrium conditions that must surround particles of incompletely reacted base, causing minerals to precipitate that are not stable in the low-pH bulk solution. A flow chart of the models is given Fig. 12. In the models, a portion of the raffinate is brought to pH 7 and annabergite and ferrihydrite are allowed to precipitate. These solids are then removed from the pH 7 solution (defined as Solution 11 in Fig. 12), which lowers the As, Ni and

Fe concentrations for this solution. The same solution, less the precipitated solids, is then mixed back with the original raffinate.

The proportions of raffinate and the pH 7 solution were estimated from measured changes in Ni concentrations in the bulk solution with increasing pH. For example, Raffinate 2 (pH 0.97) had an initial Ni concentration of 530 mg L^{-1} . At pH 2.18, the Ni concentration was 510 mg L^{-1} , indicating a loss of approximately 4% of Ni between pH 0.97 and 2.18. These differences are considered to be significant, as decreases in Ni concentration were consistently seen among all of the different experimental setups, and Ni was found in the precipitated solids derived from the low pH measurements. A mixture of 96% raffinate and 4% Solution 11 produces a Ni concentration of approximately 510 mg L^{-1} . This was considered an acceptable model fit. Redox conditions were not explicitly defined in these intermediate steps, rather the program estimated a pe value, which was between -0.55 to -0.76 .

To model the pH 3.23 solution, a mixture of 87% raffinate and 13% of the pH 7 solution was assumed. In general, as the pH increased the proportion of neutralized solution increased. These initial steps were used for all the models (Table 4). The proportions of neutralized solution were similarly increased to model the pH 4.09 and 5.29 solutions. The pH 5.29 solution required 60% raffinate and 40% of the pH 7 solution (Fig. 12). The pH 5.29 solution was the starting solution for modeling the solutions at pH 6.24 and 7.32. To model the pH 6.24 solution the pH 5.29 solution was neutralized to pH 6.24. Scorodite, gypsum, basaluminite and ferrihydrite precipitated at this pH. The pH 6.24 solution was then used as the starting composition for the final simulation. At pH 7.32, the model predicted that gypsum, theophrastrate and ferrihydrite would precipitate. Excellent agreement is observed

Table 4
Parameters used in the geochemical model and modeling results

Solution Number	pH	pe	$-\log K_{\text{sp}}$ Scorodite	Proportions: Raffinate/ High pH Solution	Measured As (mg/L)	Modeled As (mg/L)	Measured Ni (mg/L)	Modeled Ni (mg/L)
1	0.97	11.3	Undersaturated		690		530	
2	2.18	10.9	22.36	0.96/0.04	150	180	510	510
3	3.23	9.93	22.79	0.87/0.13	13	13	490	490
4	4.09	7.83	23.50	0.82/0.18	3.5	3.1	470	470
5	5.29	4.66	24.39	0.60/0.40	1.1	1	380	390
6	6.24	2.36	25.55	No Mix	0.56	0.55	240	390
7	7.32	0.0	25.55	No Mix	0.37	0.55	13	29

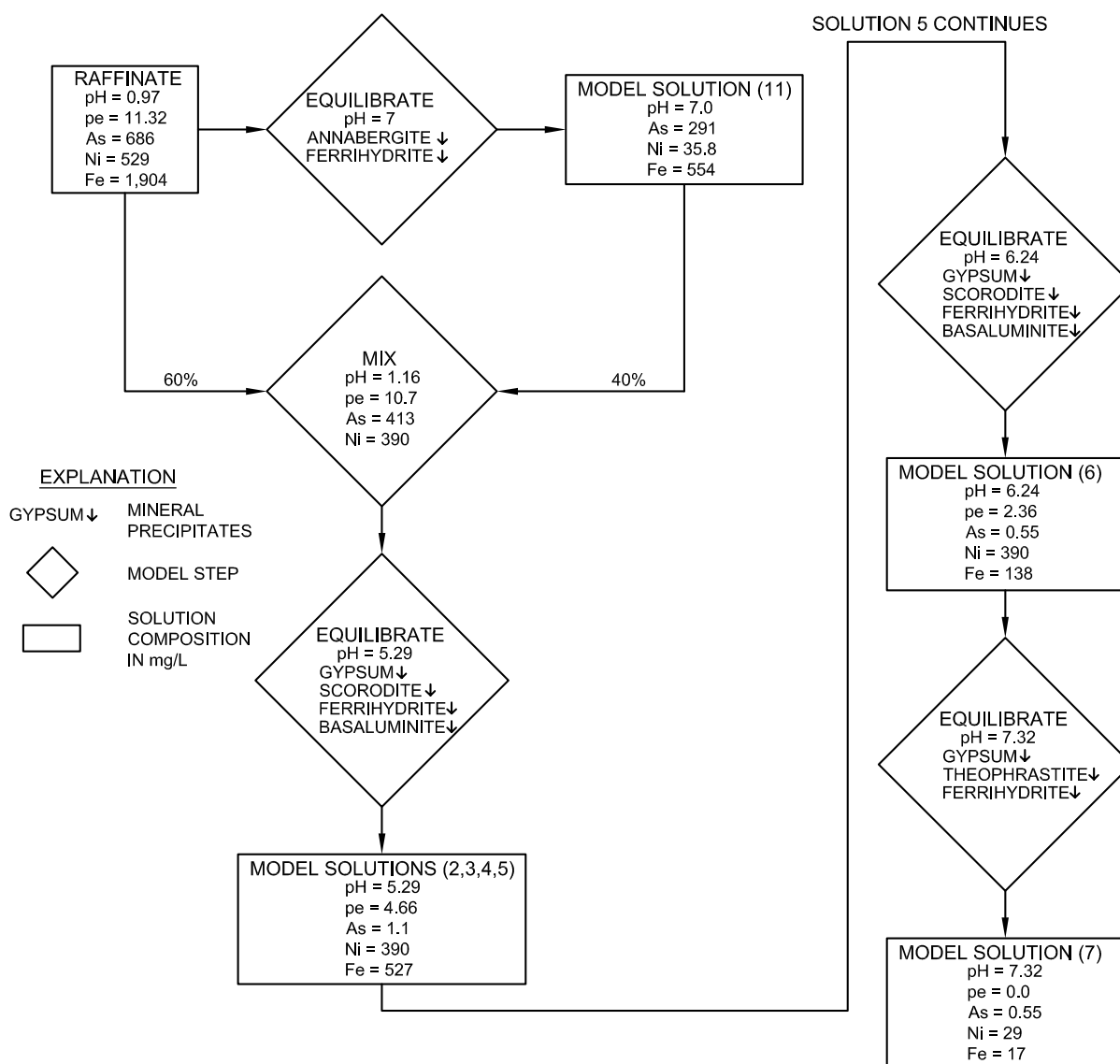


Fig. 12. Flow chart showing steps used in the geochemical model. The figure shows the conditions and resulting compositions needed to produce the final three solutions (numbers 5, 6 and 7). The pH 5.29 solution (Solution 5) is saved and provides the starting composition for Solutions 6 and 7.

between actual and modeled concentrations (Fig. 13).

Successful modeling of the raffinate neutralization process required that both equilibrium and non-equilibrium reactions be considered. To model the non-equilibrium reactions certain modeling steps and conditions were explicitly defined. Alternative model assumptions could have been chosen to produce the same final concentrations. For example, the pH for the disequilibrium step could have been set at pH 9 instead of 7. More Ni would have been removed and smaller proportions of the pH 9 solution would have been required in subsequent mixing steps. It is likely that theophrastrite rather

than annabergite precipitates in response to the pH gradients, particularly in the mid pH ranges where most of the As already has been removed. Because of its non-unique nature, the model at best provides a qualitative understanding of neutralization processes.

The model does not include any surface complexation modeling. There are several reasons why surface complexation modeling was not included. Phase rule requirements are violated if it is assumed that simultaneous equilibrium involving a precipitated phase and a “surface complexed phase” will result in an As concentration that is lower than the solubility of the precipitated phase. For such

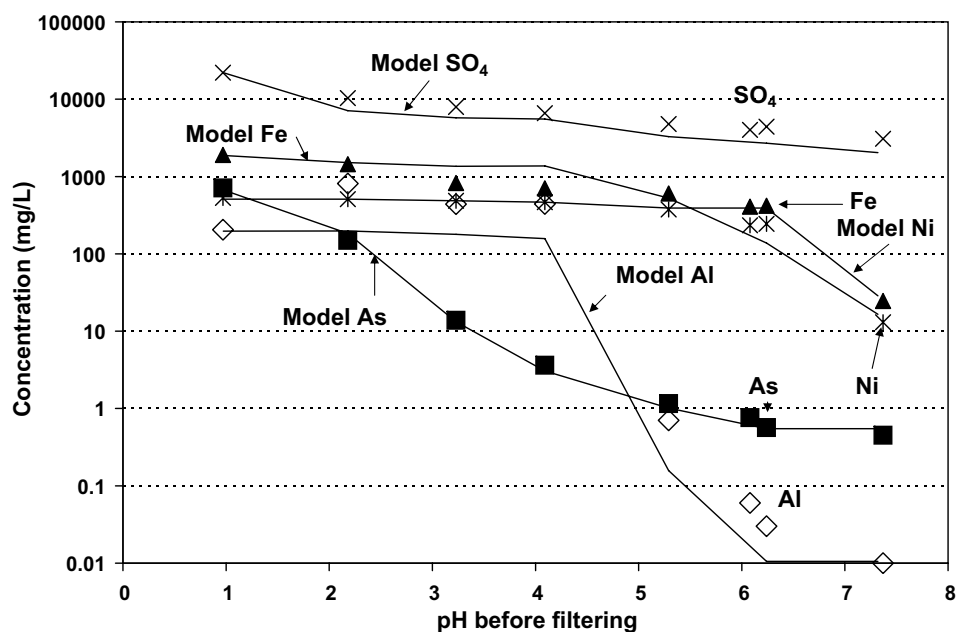


Fig. 13. Model fits (lines) of the concentration data (points) measured during neutralization of raffinate with slaked lime. Modeling assumptions and results are summarized in Table 4. Symbols: $\text{SO}_4 = \text{X}$, Fe = triangle, As = square, Ni = lined X, Al = diamond.

conditions the phase (or reaction) that equilibrates with the highest activity of As will control its concentration in solution. For example, any As released from scorodite dissolution should adsorb until the sorption capacity of the ferrihydrite is reached, and the remaining scorodite would still define the activity of dissolved As. Accordingly, for precipitation and adsorption both to apply requires that the two processes not be coupled in the same model step. Simulations that separate the processes often produce unrealistically low final concentrations.

Interaction with secondary solids does, however, play a role in the behavior of Ni. Concentrations in solution are lower than a mineral precipitation equilibrium model would predict, even when a stable $\text{Ni}(\text{OH})_2$ phase is used in the model. The difference between Ni concentrations observed in the bulk experiments and the single beaker experiments suggests that the secondary solids, such as ferrihydrite, influence Ni concentrations. Adsorption reactions may exert an influence on the final Ni concentrations in these experiments, but for reasons outlined above adsorption of Ni was not included in the model.

6. Conclusions

Previous studies have shown that elevated As and Ni concentrations in acid raffinates can be reduced to $1\text{--}2\text{ mg L}^{-1}$ or less if the molar Fe/As ratio of

the raffinate is adjusted to ≥ 3 prior to neutralization (cf. Krause and Ettel, 1985; Langmuir et al., 1999a,b). After Fe/As ratio adjustment, the raffinate/tailings slurry in the JEB mill at McClean Lake is neutralized with lime to pH 4, and then to pH 7.0–7.5 in successive neutralization tanks with residence times in each tank of about 90 min. The result is final As and Ni concentrations of 1 mg L^{-1} or less in neutralized raffinate/tailings slurries prior to their sub-aqueous disposal in a tailings management facility.

This study was designed to understand changes in the solution chemistry and mineralogy of the raffinate/tailings during neutralization in the JEB mill, with a focus on the behavior of As and Ni. Mill-produced raffinates from U ore processing were neutralized from pH 2 to 7.5 in laboratory batch tests. Study results led to the following conclusions. Neither the use of NaOH or $\text{Ca}(\text{OH})_2$ as the base, or whether primary tailings solids (leach residue) were present or absent during neutralization affected final As nor Ni concentrations. Precipitate mineralogy was determined by chemical analysis, XRD, SEM, EM, XM and EXAFS methods. Among the minerals precipitated, gypsum constituted from 71 to 83% of the total, and was at saturation ($\text{SI} = 0.05 \pm 0.13$) at all pH's.

Arsenic(III) which apparently exceeded As(V) in the raffinate, was rapidly oxidized during neu-

tralization. Annual sampling programs conducted at the JEB TMF have shown that with time As(III) is completely oxidized to As(V) in the buried tailings. Other researchers have demonstrated that the oxidation of As(III) to As(V) is facilitated through hydrated Fe(III) oxide particles (Greenleaf et al., 2003). Arsenic in the raffinate was precipitated chiefly in poorly crystalline scorodite, with smaller amounts in annabergite, and trace amounts coprecipitated or adsorbed, probably by ferrihydrite. Geochemical modeling indicated that the scorodite, most of which was precipitated between pH 2–4, decreases in solubility (increases in crystallinity) with increasing pH. Other precipitated phases included hydrobasaluminite, “green rust II”, strengite, jarosite and theophrastrate. Nickel was removed from the raffinate by precipitation in scorodite, annabergite and theophrastrate. Forward geochemical modeling supports the conclusion that the annabergite, which is always undersaturated in the bulk solutions, and some theophrastrate, which only equilibrates above pH 7, were precipitated at lower bulk solution pHs in the vicinity of particles of unreacted base where local pH values may be as high as 10–12.

Acknowledgement

This work was supported by AREVA Resources Canada, Inc. of Saskatoon, Saskatchewan, Canada.

References

- American Society for Testing and Materials, 2005. Annual book of ASTM standards 2005, v.05.06.
- Bourayne, A. de, Pollock, R., Rowson, J., 1999. Tailings management for high grade uranium ores with high arsenic and nickel content. ICEM '99 7th Internat. Conf. Radioactive Waste Mgmt. and Environmental Remediation. September 26–30, Nagoya, Japan.
- Chen, N., 2006. Pers. Comm. Canadian Light Source Inc., 101 Perimeter Rd., Saskatoon, SK, S7 N 0X4, Canada.
- Foster, A.L., Brown Jr., G.E., Tingle, T.N., Parks, G.A., 1998. Quantitative arsenic speciation in mine tailings using X-ray absorption spectroscopy. *Am. Mineral.* 83, 553–568.
- Greenleaf, J.E., Cumbal, L., Staina, I., Sengupta, A.K., 2003. Abiotic As(III) oxidation by hydrated Fe(III) oxide (HFO) microparticles in a plug flow columnar configuration. *Trans I Chem. Eng.* 81 (Part B), 1–12.
- Harris, G.B., Krause, E., 1993. The disposal of arsenic from metallurgical processes: Its status regarding ferric arsenate. Paul E. Queneau Internat. Symp. “Extractive Metallurgy of Nickel, Cobalt and Associated Metals”. TMS Ann. Meeting, Denver, CO, USA, February 21–25.
- Harris, G.B., Monette, S., 1988. The stability of arsenic-bearing residues. In: Reddy, R.G., Hendrix, J.L., Queneau, P.B. (Eds). *Proc. Symp. “Arsenic Metallurgy Fundamentals and Applications”*. TMS Annual Meeting & Exhibition. Phoenix, AZ, (Jan 25–28). 469–488.
- JCPDS, 2005. Joint committee for powder diffraction standards. Intl. Center for Diffraction Data, Newtown Square, PA, 19073, USA.
- Krause, E., Ettl, V.A., 1985. Ferric arsenate compounds: are they environmentally safe? Solubilities of basic ferric arsenates. In: Oliver, A.J. (Ed.). *Impurity Control and Disposal, 15th Ann. Meeting, Canadian Inst. Mining, Metallurgy & Petroleum*. Montreal, Canada, 5/1–5/20.
- Langmuir, D., 1997. *Aqueous Environmental Geochemistry*. Prentice Hall, Upper Saddle River, NJ.
- Langmuir, D., Mahoney, J.J., MacDonald, A.K., Rowson, J., 1999a. Predicting the arsenic source-term from buried uranium mill tailings. *Proc. Tailings and Mine Waste '99*. Fort Collins, Colorado, pp. 503–514.
- Langmuir, D., Mahoney, J., MacDonald, A., Rowson, J., 1999b. Predicting arsenic concentrations in the porewaters of buried uranium mill tailings. *Geochim. Cosmochim. Acta* 63, 3379–3394.
- Langmuir, D., Mahoney, J., Rowson, J., 2006. Solubility products of amorphous ferric arsenate and crystalline scorodite ($\text{FeAsO}_4 \cdot 2\text{H}_2\text{O}$) and their application to arsenic behavior in buried mine tailings. *Geochim. Cosmochim. Acta* 70, 2942–2956.
- Macalady, D.L., Langmuir, D., Grundl, T., Elzerman, A., 1990. Use of model generated Fe^{3+} ion activities to compute Eh and ferric oxyhydroxide solubilities in anaerobic systems. In: Melchior, D.C., Bassett, R.L. (Eds). *Chemical Modeling in Aqueous Systems II*. Am. Chem. Soc. Symp. Ser. 416. Am. Chem. Soc. Washington, DC. 350–367.
- Mahoney, J., Langmuir, D., Gosselin, N., Rowson, J., 2005. Arsenic readily released to pore waters from buried mill tailings. *Appl. Geochem.* 20, 947–959.
- Moldovan, B.J., Hendry, M.J., 2005. Characterizing and quantifying controls on arsenic solubility over a pH range of 1–11 in a uranium mill-scale experiment. *Environ. Sci. Technol.* 39, 4913–4920.
- Moldovan, B.J., Jiang, D.T., Hendry, M.J., 2003. Mineralogical characterization of arsenic in uranium mine tailings precipitated from iron-rich hydrometallurgical solutions. *Environ. Sci. Technol.* 37, 873–879.
- Paktunc, D., Foster, A., Heald, S., Laflamme, G., 2004. Speciation and characterization of arsenic in gold ores and cyanidation tailings using X-ray absorption spectroscopy. *Geochim. Cosmochim. Acta* 68, 969–983.
- Paktunc, D., Foster, A., Laflamme, G., 2003. Speciation and characterization of arsenic in Ketz River Mine Tailings using x-ray absorption spectroscopy. *Environ. Sci. Technol.* 37, 2067–2074.
- Paktunc, A.D., Szymanski, J., Lastra, R., Laflamme, J.H.G., Enns, V., Soprovich, E., 1998. Assessment of potential arsenic mobilization from the Ketz River mine tailings, Yukon, Canada. In: Petruk, W. (Ed.), *Waste Characterization and Treatment*. Soc. Mining Metallurgy & Exploration, Inc., pp. 49–60.

- Parkhurst, D.L., Appelo, C.A.J., 1999. User's guide to PHREEQC (Version 2), A computer program for speciation, batch-reaction, one-dimensional transport, and inverse geochemical calculation. U.S. Geol. Surv. Water-Resour. Invest. Rep., 99–4259.
- Pichler, T., Hendry, M.J., Hall, G.E.M., 2001. The mineralogy of arsenic in uranium mine tailings at the Rabbit Lake in-pit facility, northern Saskatchewan, Canada. *Environ. Geol.* 40, 495–506.
- Riveros, P.A., Dutrizac, J.E., Spencer, P., 2001. Arsenic disposal practices in the metallurgical industry. *Can. Metall. Quart.* 40, 395–420.
- Roussel, C., Neel, C., Bril, H., 2000. Minerals controlling arsenic and lead solubility in an abandoned gold mine tailings. *Sci. Total Environ.* 263, 209–219.
- Slaughter, M., 1985. Method for determining composition and amount of minerals in rocks and soils. *Nat. and Intat. Clay Conf.: Workshop Manual on Quantitative Analysis of Clays*.
- Slaughter, M., 1990. Quantitative determination of clays and other minerals in rocks. In: Pevear, D.R., Mumpton, E.A. (Eds.), *Clay mineral society workshop lectures, Quantitative Mineral Analysis of Clays*, vol. 1. Clay mineral Society, Evergreen, Colorado, pp. 20–151.
- Stumm, W., Morgan, J.J., 1996. *Aquatic Chemistry – Chemical Equilibria and Rates in Natural Waters*, third ed. Wiley, Interscience, New York.
- Tan, L.K., Dutrizac, J.E., 1985. Determination of arsenic(V) and arsenic(III) in ferric sulfate-sulfuric acid leaching media by ion chromatography. *Anal. Chem.* 57, 2615–2620.